

3D SEGMENTED MODEL OF HEAD FOR MODELLING ELECTRICAL ACTIVITY OF BRAIN

Egill A. Friðgeirsson^{(a),(b)}, Paolo Gargiulo^{(a),(b)}, Ceon Ramon^{(b),(d)}, Jens Haueisen,^(c)

^(a) Department of Development and Consultancy UTS

^(b) Department of Biomedical Engineering, University of Reykjavik

^(c) Institute of Biomedical Engineering and Informatics, Technical University Ilmenau, Germany

^(d) Department of Electrical Engineering, University of Washington, United States

^{(a),(b)} egillf05@ru.is, ^{(a),(b)} paologar@landspitali.is, ^{(b),(d)} ceonramon@yahoo.com, ^(c) jens.haueisen@tu-ilmenau.de

ABSTRACT

Computer simulation and modelling of the human body and its behaviour are very useful tools in situations where it is either too risky to perform an invasive procedure or too costly for in vivo experiments or simply impossible for ethical reasons. In this paper we describe a method to model the electrical behaviour of human brain from segmented MR images. The aim of the work is to use these models to predict the electrical activity of the human brain under normal and pathological conditions. The image processing software package MIMICS is used for 3D volume segmentation of MR images. These models have detailed 3D representation of major tissue surfaces within the head, with over 12 different tissues segmented. In addition, computational tools in Matlab were developed for calculating normal vectors on the brain surface and for associating this information to the equivalent electrical dipole sources as an input into the model.

Keywords: Segmentation, EEG modelling; Finite element; Realistic head model.

1. INTRODUCTION

The relationship between neuronal sources and the recorded scalp electroencephalograms (EEG's) has for a long time been of interest (Abraham and Marsan 1958). This relationship is characterized by the spread of electrical currents in inhomogeneous tissues, which govern the scalp electrical potentials.

Forward EEG modelling is a discipline which uses numerical techniques such as finite element method (FEM) modelling to study the relationship between electric sources in the brain and the resulting electrical potentials at the scalp (Hallez and Vanrumste 2007). Sources in the form of current dipoles are placed in the brain and then the FEM equations are solved for the resulting potential at the scalp.

For accurate forward EEG modelling detailed segmentation of tissues is needed, especially between the electrical source and scalp. In former studies the model complexity, or the number of tissue types, has been shown to affect the results (Ramon 2006). These

have emphasized the role of accurate segmentation of the cerebrospinal fluid (CSF) and bone (Ramon 2004).

The kind of 3D segmentation used here with the software platform MIMICS (Materialize Inc, USA) has previously been applied to monitor quadriceps femoris in paraplegic patients undergoing electrical stimulation as described in (Gargiulo 2010; Gargiulo 2011).

In this work we develop high (1.0 mm) resolution human head models from segmented MR images. These models have a detailed 3D representation of major tissue surfaces with over 12 tissue types defined.

Brain geometry is then used to locate the position and orientation of the cortical neurons to use as sources in the models. The cortical pyramidal neurons are thought to make up most of the EEG signal (Linás and Nicholson 1974; Okada 1982).

We will use these FEM models to simulate electrical activity of brain under normal and pathological conditions.

2. MATERIAL AND METHODS

2.1 MR data

A whole head T1 weighted volumetric MR scan of an adult female subject was used for this work. Each slice has 256×256 pixels, and each pixel has a gray value within the 4096 gray-scale values, meaning that it is represented with a 12-bit value. The contiguous slice thickness was 1.0 mm and pixel resolution was 1.0 mm. A total data set from a single scan is therefore $(256 \times 256 \times 192 \times 12)/8 = 1.9 \times 10^7$ bytes. This data set gives a complete 3D description of the tissue within the head.

2.2 Segmentation of the head

We develop detailed 3D representation of major tissues within the head including white and gray matter, cerebellum, CSF, cortical and trabecular bone, dura layer, skin, eyes and crystalline lens and so on. Some of these tissues have a distinguished threshold while other are displayed within the same gray values interval. In these cases special segmentation techniques and manual editing are employed to isolate single tissues from the surroundings.

The process starts from a cross section where the selected tissue boundaries are well visible. A contour is manually drawn around the region of interest (ROI) and projected to the next cross sections in both directions. If the contour fits well the new cross sectional area then it is projected unchanged forward to the next slice, otherwise it is adapted using manual editing and then projected ahead to the next slice. If the cross sectional area doesn't change much between slices it is enough to identify the contour in only a few slices and interpolate between them. This process continues until all cross sections containing the selected ROI are covered. The contour areas are then erased creating a gap between the ROI and the surroundings. Finally, a new segmentation mask representing ROI is created applying a region growing procedure which creates a new mask separating the edited structure that is no longer connected to the surrounding tissues.

Some tissues like the dura layer and the skin were segmented using other tools in mimics. The dura layer was segmented using wrapping functions on the CSF tissue mask. Similarly the skin was segmented using a wrapping function on the soft tissue mask.

The result of the segmentation process and a 3D rendering thereof is shown in Fig.1.

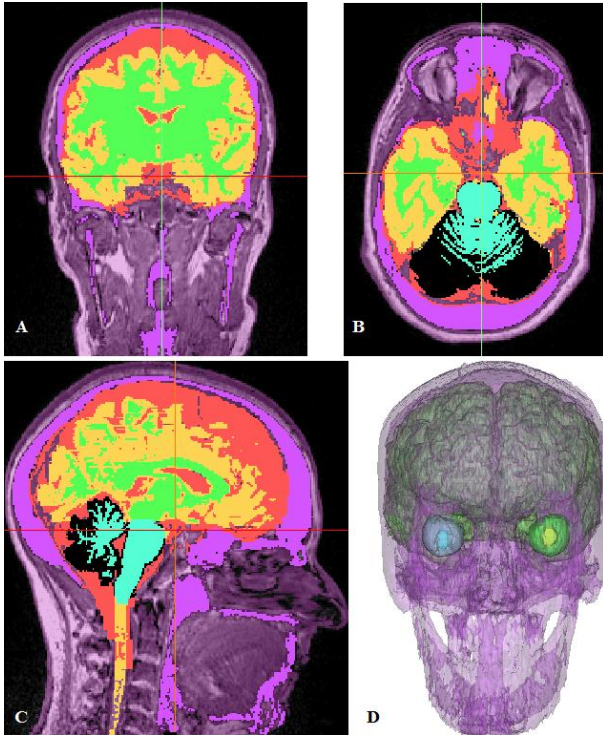


Figure 1: Segmentation results showing different tissue surfaces. Coronal view (A), axial view (B), sagittal view (C) and 3-D reconstruction of the segmented tissues (D).

2.3 Normal vectors

After the head has been adequately segmented the next step is to locate the surface boundary between the white and gray matter. This was done by using isosurface

algorithms in Matlab version 7.10 (Mathworks Inc, USA) with a binary image matrix with one as the white matter and zero elsewhere.

After the surface nodes were extracted, normal vectors were computed using the central finite difference approximation to the numerical gradient at those nodes in the binary matrix. So for each surface node $f(x, y, z)$ the three gradient components are found by (1):

$$\begin{aligned}\frac{\partial f}{\partial x} &= f\left(x + \frac{h_x}{2}\right) - f\left(x - \frac{h_x}{2}\right) \\ \frac{\partial f}{\partial y} &= f\left(y + \frac{h_y}{2}\right) - f\left(y - \frac{h_y}{2}\right) \\ \frac{\partial f}{\partial z} &= f\left(z + \frac{h_z}{2}\right) - f\left(z - \frac{h_z}{2}\right)\end{aligned}\quad (1)$$

Where h_x , h_y and h_z are the separation between the adjacent points in x, y and z directions, respectively.

Since the surface nodes represent a level set the gradient components are perpendicular to the surface and are therefore the normal vector components. This can be seen in Fig 2.

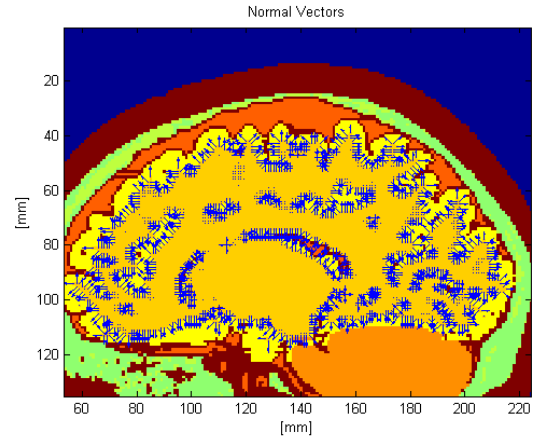


Figure 2: The normal vectors within a segmented slice of the brain.

2.4 Electrical Activity Modelling

An example of modelling the spontaneous electrical activity of the normal brain is presented here using the normal vectors to represent location and orientation of dipoles. A FEM model was constructed out of 192 segmented axial slices extending from top of the head to the bottom of the neck. The voxel resolution was $1 \times 1 \times 1$ mm. The electrical conductivities of various tissues were obtained from the literature and are summarized in our previous work (Ramon 2006). The conductivity of the dura matter is not well established and it was found to have a large range from 0.02 to 0.1 S/m (Oozeer 2005). For our work, we used a midrange value of 0.06 S/m.

The electrical activity in the top portion of the brain, above the eye level, was simulated with 125 dipoles randomly located in different parts of the brain. The dipole intensity distribution was in the range of 0.0 to 0.4 mA meter with a uniform random distribution.

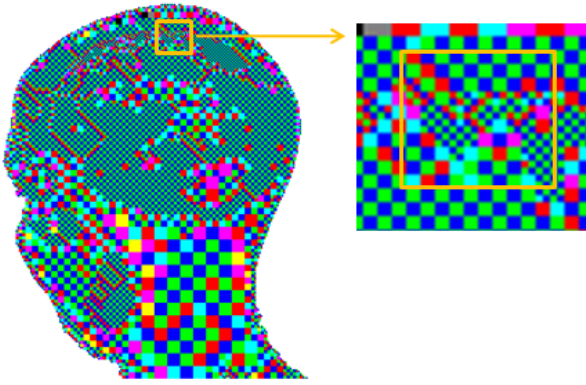


Figure 3: The FEM mesh of the adaptive solver.

An adaptive FEM solver, developed by us (Schimpf et al. 1998; Ramon et al. 2006), was used to compute flux and potential distribution in the whole head model. Fig. 3 shows an adaptive FEM grid and the details of the grid in the vicinity of one of the dipolar source. It shows an adaptive FEM grid and the details of the grid in the vicinity of one of the dipolar source. The FEM software automatically adjusts the grid resolution in each pass to achieve the desired L2 norm while keeping the computational errors to a minimum level.

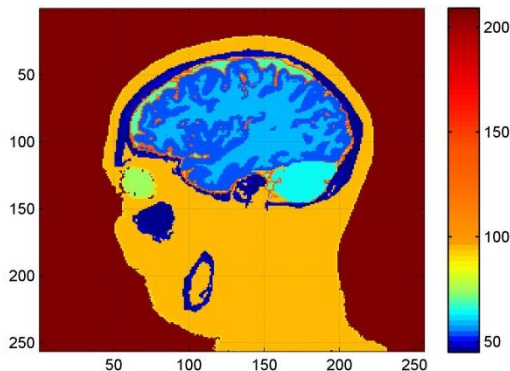


Figure 4: The segmented anatomical slice.

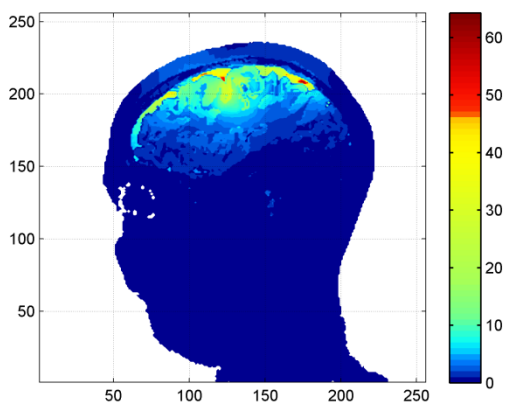


Figure 5: Current density distribution within the segmented slice. The intensity scale is in $\mu\text{A}/\text{cm}^3$. The nose is on the top.

An example of the current distribution is given in Figs. 4 and 5. The Fig. 4 shows the segmented anatomical slice and Fig. 5 shows the volume current density distribution. The current flow pattern follows the anatomical tissue boundaries very accurately. This is very pronounced at the CSF, gray and white matter boundaries. This shows that our segmentation and FEM modelling works well for computing flux and potential distributions in human head models.

2.5 Differential Contributions of Dipolar Activity to Scalp Potentials

The above described tools were used to analyze how neuronal activity at different depths contribute towards scalp EEGs. For this purpose we computed the scalp potentials due to dipoles in two layers at two different depths. The first layer, called Layer 1, was from top of the brain surface to the depth of 0.3 cm and the second layer, called Layer 2, was from the depth of 0.3 to 0.6 cm from top of the brain surface. There were 820 dipoles in the first layer and 3780 dipoles in the second layer. The total number of dipoles was 4,600. The dipole intensity distribution was in the range of 0.0 to 0.4 mA meter with a uniform random distribution.

The adaptive FEM solver described above was used to compute flux and potential distribution in the whole head model. Two models were studied. For one model the dipoles in the first layer were used and in the other model the dipoles in the second layer were used. The scalp potentials were extracted from the node potentials in the finite element models of the head. All computations were performed on an Intel quad core, second generation, 2.4 GHz workstation with 8 GB memory. Each run took about 10 minutes. Post-processing and visualizations were done using Matlab software, version 7.10.

3 RESULTS

Scalp potentials due to the first and second layers are given in Fig. 6 and a combination of both layers are given in Fig. 7. The scalp potentials of Layer 1 and Layer 2 both have an equivalent dipolar activity patterns. For the Layer 1, the positive contours are on the left side and the negative contours are on the right side and zero-crossing line of yellow colour is almost vertical in the middle of the positive and negative contours. An equivalent dipolar source can visualized as extending from the centre of the negative contours to the centre of the positive contours. For the Layer 2, almost circular negative contours are visible in the plot. This will suggest that the equivalent dipolar activity is pointing from the top to the bottom of the head, i.e., from superior to inferior position. The combined activity of the dipolar sources in Layer 1 and Layer 2 is given in Fig. 7 and it shows that it is dominated by the scalp potentials due to dipoles in Layer 2. This is feasible because there are 3780 dipoles in Layer 2 as compared with only 820 dipoles in Layer 1.

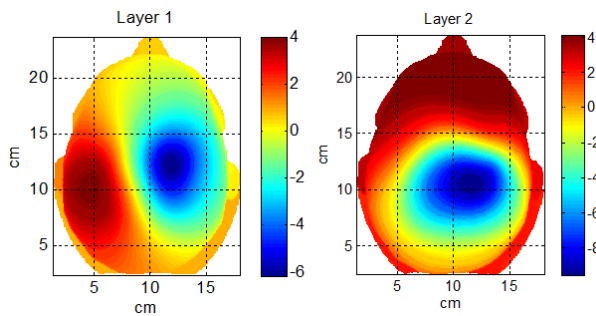


Figure 6: Scalp potentials due to dipoles in layers 1 and 2. The magnitude scale of the colour bar is in micro volts (μV).

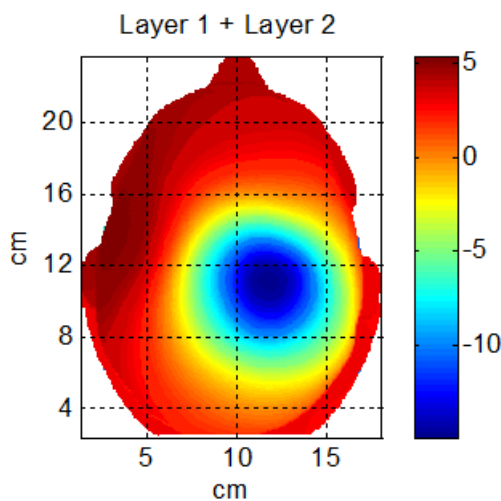


Figure 7: Scalp potentials due to combined dipolar activity from layer 1 and 2. The nose is on the top. The magnitude scale of the colour bar is in micro volts (μV).

4 CONCLUSION

These are our preliminary results to show our capabilities to segment the tissue boundaries with the use of the MIMICS software, to build detailed accurate anatomical models and to accurately compute current and potential distributions in the model. An application of our tools for differential contributions of the dipolar activity to the scalp potentials is also presented. In future, we plan to use these tools for modelling of the electrical activity of the brain under normal and pathological conditions and to research the influence of different brain structures on the EEG signal.

ACKNOWLEDGMENTS

This work has been supported by the University Hospital Landspítali research fund.

REFERENCES

- Abraham K. and Marsan C.A., 1958. Patterns of cortical discharges and their relation to routine scalp electroencephalography, *Electroencephalography and Clinical Neurophysiology* 10(3):447-461.
- Gargiulo, P., Kern, H., Carraro, U., Ingvarsson, P., Knútsdóttir, S., Guðmundsdóttir, V., Yngvason,

S., Vatnsdal, B. and Helgason, T., 2010. Quantitative color 3-dimensional computer tomography imaging of human long-term denervated Muscle. *Neurological Research* 32:13-20

- Gargiulo, P., Vatnsdal, B., Ingvarsson, P., Knútsdóttir, S., Guðmundsdóttir, V., Yngvason, S. and Helgason, T., 2008. Restoration of Muscle Volume and Shape Induced by Electrical Stimulation of Denervated Degenerated Muscles: Qualitative and Quantitative Measurement of Changes in Rectus Femoris Using Computer Tomography and Image Segmentation. *Artificial Organs* 32: 609–613.

- Hallez, H., Vanrumste, B., Grech, R., Muscat, J., De Clercq, W., Verguult, A., D'Asseler, Y., Camilleri, K.P., Fabri, S.G., Van Huffel, S. and Lemahieu, I. 2007. Review on solving the forward problem in EEG source analysis. *Journal of Neuroengineering and Rehabilitation* 4: 46.

- Linás, R.R., Nicholson, C., 1974. Analysis of field potentials in the central nervous system. *Handbook Electroencephalography Clinical Neurophysiology* 2B:61-83.

- Okada, Y.C., 1982. Neurogenesis of evoked magnetic fields. In: Williamson, S.J., Romani, G.L., Kaufman, L. & Modena, L., eds. *Biomagnetism; an Interdisciplinary Approach*. New York:Plenum Press, 399-408,

- Oozeer M., Veraart, C., Legat, V., Delbeke, J., 2005. Simulation of intra-orbital optic nerve electrical stimulation. *Medical and Biological Engineering Computing* 43(5):608-17.

- Ramon, C., Schimpf, P.H., Haueisen, J., Holmes, M, and Ishimaru, A., 2004, Role of soft bone, CSF and gray matter in EEG simulations. *Biomedical Engineering Online* 16(4):245-8

- Ramon, C., Schimpf, P.H and Haueisen, J., 2006. Influence of head models on EEG simulations and inverse source localizations. *Biomedical Engineering Online* 5:10

- Schimpf PH, Haueisen J, Ramon C, and Nowak H., 1998. Realistic computer modeling of electric and magnetic fields of human head and torso. *Parallel Computing* 24:1433-1460.

AUTHORS BIOGRAPHY

Egill Axfjord Fridgeirsson is a 24 year old master student at Reykjavik University Iceland in Biomedical Engineering. He is on his second year of graduate studies and this work represents part of his master thesis. His research interests are Medical modeling, Biomagnetism and clinical applications of medical models. He currently works in the Clinical Engineering department of Landspítali University hospital.

Paolo Gargiulo is assistant professor at Reykjavik University and works as biomedical engineer and researcher at the University Hospital of Iceland. He studied electrical engineering at University Federico II

in Naples, and obtained a PhD at Technical University of Vienna, Austria. His research interests are in the field of electrical stimulation medical modeling and rapid prototyping for clinical applications.

Ceon Ramon obtained his Ph.D. in Electrical Engineering from University of Utah in 1973 specializations in lasers and quantum optics. For the past 20 years, his research efforts have been largely involved with neuroscience and the developmental genesis of human EEG under normal and epileptic conditions. For the past 40 years, Ceon has held teaching and research appointments at the University of Utah, State University of New York, Stony Brook and at the University of Washington. Presently, he is an Affiliate Professor of Electrical Engineering at the University of Washington and a Professor of Biomedical Engineering at Reykjavik University, Iceland.

Jens Haueisen received a M.S. and a Ph.D. in electrical engineering from the Technical University Ilmenau, Germany, in 1992 and 1996, respectively. From 1996 to 1998 he worked as a Post-Doc and from 1998 to 2005 as the head of the Biomagnetic Center, Friedrich-Schiller-University, Jena, Germany. Since 2005 he is Professor of Biomedical Engineering and directs the Institute of Biomedical Engineering and Informatics at the Technical University Ilmenau, Germany. His research interests are in the numerical computation of bioelectric and biomagnetic fields and biological signal analysis.